

# Lifetime measurements in the transitional nucleus $^{150}\text{Sm}$

<sup>1</sup>S. P. Bvumbi, <sup>1</sup>S. H. Connell, <sup>2</sup>J. F. Sharpey-Scafer, <sup>3</sup>S. M. Mullins,  
<sup>3</sup>R. A. Bark, <sup>3</sup>E. A. Lawrie, <sup>3</sup>J. J. Lawrie, <sup>1</sup>P. L. Masiteng, <sup>3,4</sup>S. S.  
Ntshangase and <sup>2,3</sup>O. Shirinda

<sup>1</sup>University of Johannesburg, Department of Physics, P. O. Box 524, Auckland Park 2006,  
South Africa

<sup>2</sup>University of the Western Cape, South Africa

<sup>3</sup>iThemba LABS, South Africa

<sup>4</sup>University of Zululand, South Africa

E-mail: [suzanb@uj.ac.za](mailto:suzanb@uj.ac.za)

**Abstract.** Weakly populated band structures have been established in the nucleus  $^{150}\text{Sm}$  at low to medium spins following the  $^{136}\text{Xe}(^{18}\text{O}, 4n)^{150}\text{Sm}$  fusion evaporation reaction at 75 MeV. The band built on the second  $0^+$  state has been established. Lifetime measurements have been performed by the Doppler Shift Attenuation method in the positive-parity S-band. Experimental transition strengths  $B(E2)$  together with angular-intensity ratios and linear polarization were measured. The preliminary results support the strong collective interpretation.

## 1. Introduction

The nucleus  $^{150}_{62}\text{Sm}_{88}$  lies in a transitional region where nuclear collectivity rapidly changes from vibrational to rotational motion [1]. This is reflected in the rapid change in the experimental  $\frac{E(4^+)}{E(2^+)}$  energy ratios between  $N = 86$  and  $N = 96$  nuclei for isotopes with  $Z \sim 64$ , as shown in Fig 1. The  $\frac{E(4^+)}{E(2^+)}$  ratios of 2.00, 2.50 and 3.33 are expected for pure vibrational,  $\gamma$ -soft and rotational, respectively. The ratio  $\frac{E(4^+)}{E(2^+)}$  for  $^{150}\text{Sm}$  is  $\sim 2.32$  approaching 2.50, the value expected for a  $\gamma$ -soft rotor [2]. The structure of the nucleus  $^{150}\text{Sm}$  is very complex and extracting lifetimes is a useful approach because this gives information on the reduced electromagnetic transition rates which are very sensitive to the intrinsic structure of the excited states. From these measurements, information on the deformation of the different collective structures in a deformed nucleus may be obtained.

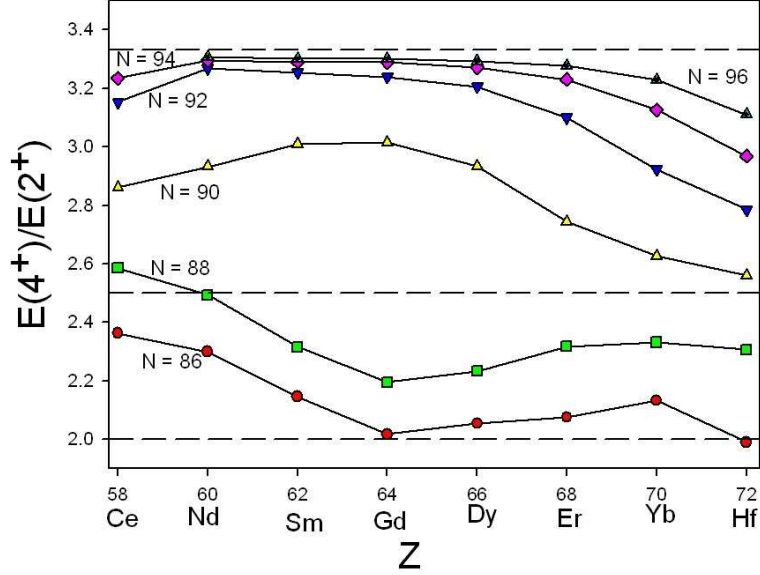


**Figure 1.**  $\frac{E(4^+)}{E(2^+)}$  energy-ratio systematics for even-even nuclei as a function of atomic number  $Z$ . The horizontal dashed lines represent limits expected for pure vibrational (2.00), rotational (3.33), and  $\gamma$ -soft (2.50) behaviour.

## 2. Experimental details and Results

The high spin states of the nucleus  $^{150}\text{Sm}$  were populated using the  $^{136}\text{Xe}(^{18}\text{O}, 4n)^{150}\text{Sm}$  fusion evaporation reaction. It was studied at iThemba LABS, using the AFRODITE spectrometer array equipped with 9 clover HPGe detectors in BGO shields. An  $^{18}\text{O}$  beam energy of 75 MeV was used to bombard  $\sim 5 \text{ mg}\cdot\text{cm}^{-2}$  of frozen  $^{136}\text{Xe}$  target, backed by a  $1 \text{ mg}\cdot\text{cm}^{-2}$  layer of  $^{197}\text{Au}$ . A total of  $\sim 5 \times 10^8$  events was accumulated over 3 days of beam time. The trigger condition was such that two Compton-suppressed HPGe detectors fired in prompt time coincidence. The data was unfolded into a two-dimensional matrix which was analyzed using Radware [3]. The decay scheme obtained from our data is shown in Fig. 2. In order to extract lifetimes in the excited levels in  $^{150}\text{Sm}$  we used the doppler shift attenuation method (DSAM) [4]. This method senses the lifetime of the nuclear level by careful modelling of the velocity dependent doppler shift of the emitted photon. The recoiling nucleus slows down on a time scale that correlates with different velocity distributions for different nuclear level lifetimes. It requires a good knowledge of the material in which the recoiling nucleus comes to rest. The analysis is further assisted by viewing the recoiling nucleus from several different angles, (forward, perpendicular and backward with respect to the average recoil directions), as this allows a more robust modelling of the DSAM lineshapes.

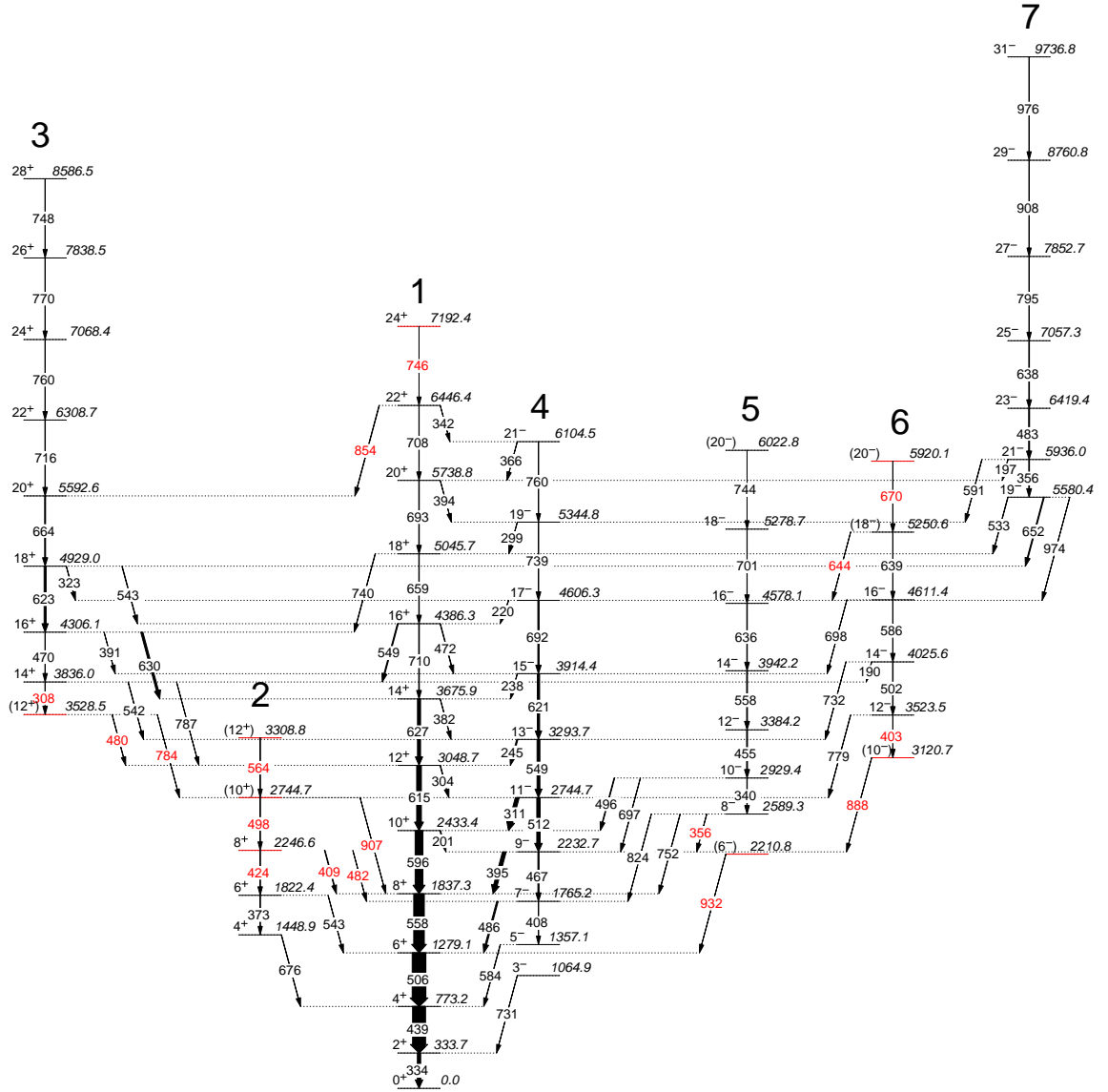


**Figure 2.** The new level scheme for  $^{150}\text{Sm}$  obtained from our  $^{136}\text{Xe}(^{18}\text{O}, 4n)^{150}\text{Sm}$  reaction with new levels and  $\gamma$ -rays in red. The levels with spin and parity in parentheses represent levels whose spins and parities could not be determined due to lack of statistics.

### 2.1. New levels in $^{150}\text{Sm}$

The new levels observed in this work are shown in Fig. 2. Three weakly populated bands 2, 5 and 6 have been observed in  $^{150}\text{Sm}$ . Previously, states up to  $6^+$  were observed in band 2 and the current work has observed three additional levels from  $8^+$  to  $(12^+)$ . Levels in bands 5 and 6 are reported in the nuclear data base, however their origins cannot be traced and previous studies done by [5] did not observe this states, we therefore consider them new observations. Two new states have been added in band 6, making its band-head to be at energy 3120.7 keV with spin-parity  $(10^-)$ . Band 6 decays only to the lowest-negative parity band via a series of  $\Delta I = 1$  transitions. Bands 2 and 5 decay to the ground-state band via a series of  $\Delta I = 0$  transitions. Recently band 2 has been reported by [6] to have  $\Delta I = 1$  decays to the lowest-negative parity

band 4. In order for us to make firm spin and parity assignments to the transitions in the level scheme, angular-correlation measurements [7] using the directional correlation from oriented states (DCO) and linear polarization anisotropy [8] techniques were used.

## 2.2. Lifetime measurements

The lifetime measurements we made were more complicated due to the imperfect knowledge of the target thickness and absence of forwards ( $45^\circ$ ) spectra. Xenon targets gradually sublime under irradiation and without knowledge of the exact target thickness distribution during the experiment DSAM measurements are less precise. There are further complications due to complex spectra arising from some contamination, we illustrate this in Fig. 3. Our statistics allowed us to make measurements for lifetimes of the  $20^+$  and  $22^+$  states of band 3. The recoil stopping times in solid Xe and Au differ by a factor of four. At  $3 \text{ mg/cm}^2$  of Xe, recoils are stopped mainly in the target with low stopping power, while at  $1 \text{ mg/cm}^2$  they are stopped mainly in the Au backing with high stopping power. Correspondingly, for the 664 keV lineshape analysis, the difference in lifetime obtained is very large. Peaks in  $^{150}\text{Sm}$  are strongly contaminated by other known lines or unknown background peaks, and as a result only a lifetime limit can be obtained. Similarly for the 716 keV transition, this peak is contaminated by two known lines, the 710 keV and 708 keV transitions in the ground state band 1. The lifetimes we obtain are different as well, however, the uncertainty could be removed if  $45^\circ$  spectra were measured. When the lifetime of an excited state is known, its experimental strength  $B(E2)$  can be evaluated as [9],

$$B(E2) = \frac{0.05659}{t_{\frac{1}{2}}(E2)(E_\gamma)^5}(\text{eb})^2, \quad (1)$$

where  $t_{\frac{1}{2}}$  is the half-life of the E2 transition and  $E_\gamma$  is the energy of the E2 transition. With estimates of the thickness target we obtained limits of 0.45 ps and 1.3 ps for the 716 keV transition de-exciting the  $22^+$  level of band 3, and limits of 1.15 ps and 2 ps for the 664 keV transition de-exciting the  $20^+$  level in the same band, see Fig. 5 and Fig. 4. With these lifetimes estimates we get  $B(E2)$  values of  $0.668 (\text{eb})^2$  and  $0.231 (\text{eb})^2$  for the 716 keV transition respectively, and for the 664 keV transition we get  $B(E2)$  values of  $0.398 (\text{eb})^2$  and  $0.219 (\text{eb})^2$  respectively. The  $B(E2)$  values of the 716 keV and 664 keV transitions differ by a factor of three due to the different lifetimes. The estimates of the target thickness were made using Monte Carlo simulation codes COMPA, GAMMA, and SHAPE [4].

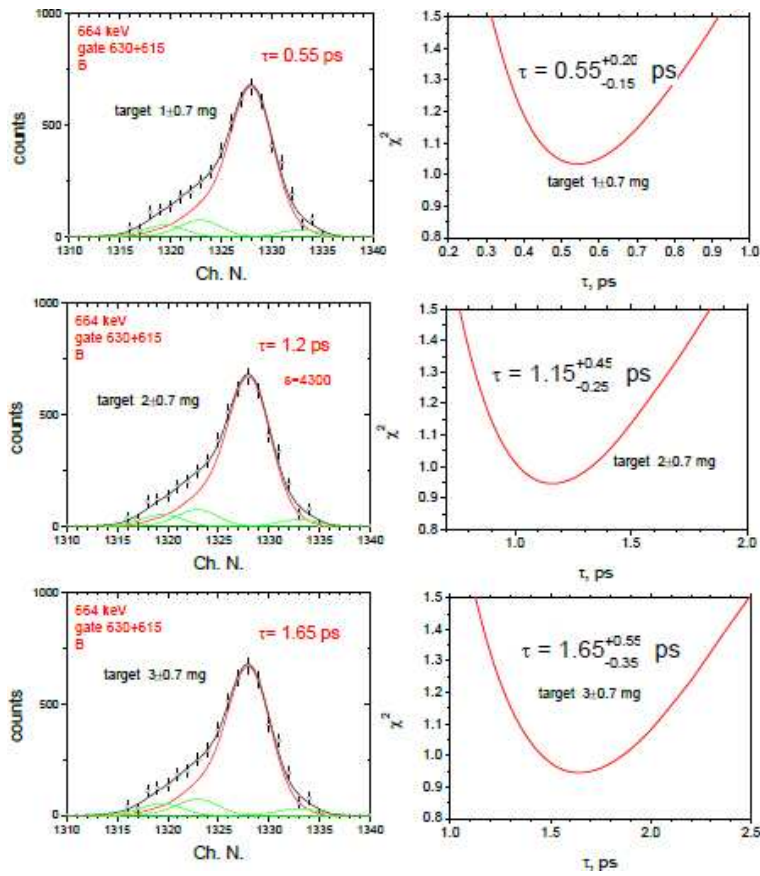


**Figure 3.** Lineshape analysis of the 664 keV peak and illustration of target thickness control during the experiment. The target thickness is evaluated by the lineshape observed.

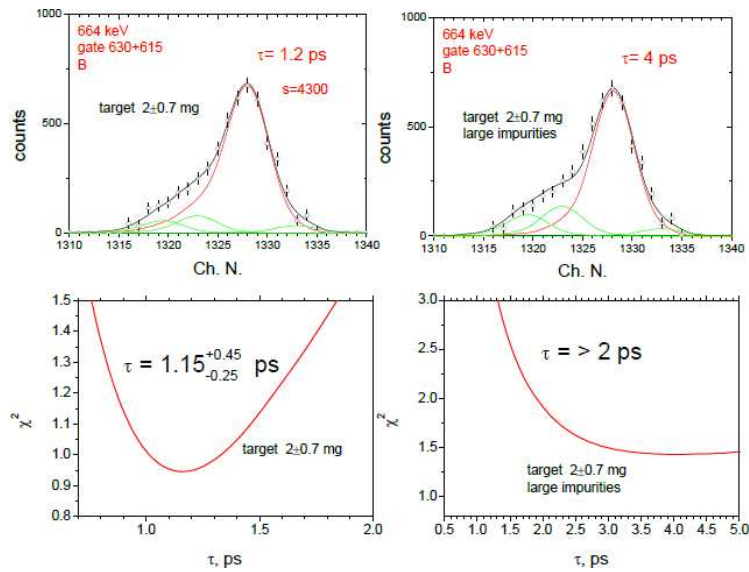


**Figure 4.** The lineshape analysis of the 664 keV transition from the  $20^+$  state of band 3 at  $135^\circ$  and the obtained lifetimes.

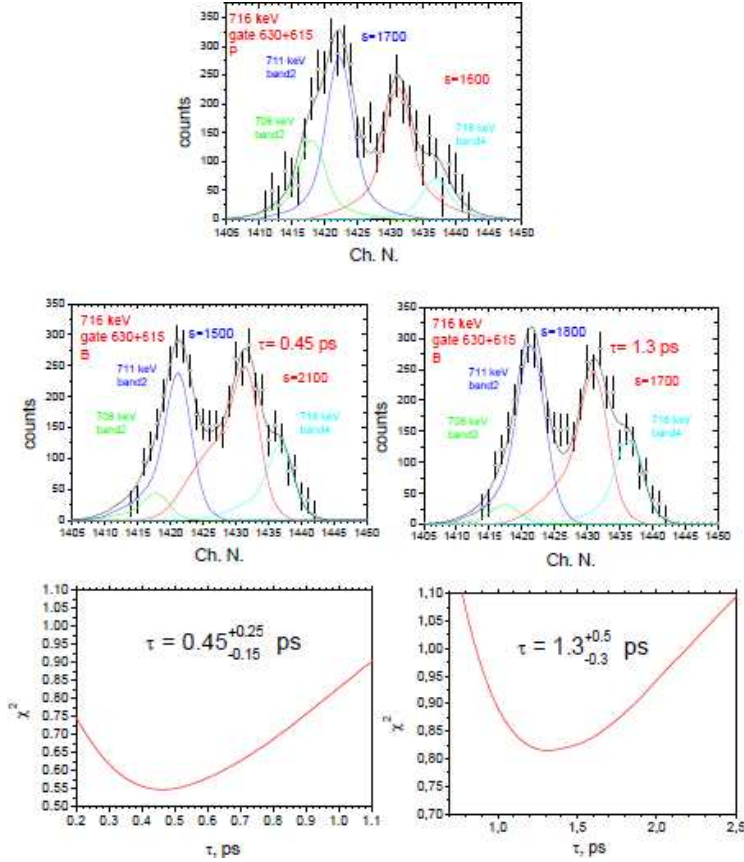


**Figure 5.** The lineshape analysis of the 716 keV transition from the  $22^+$  state of band 3 at  $135^\circ$  and the obtained lifetimes.

### 3. Discussion

The lowest levels of band 2 were originally associated with a  $K^\pi = 0^+$   $\beta$ -vibrational band [10]. However the low excitation energy of the  $0^+$  band-head has led to the questioning of this interpretation by [11]. In this reference they are interpreted as a second vacuum ( $0_2^+$ ) coexisting with the first  $0_1^+$  ground state vacuum caused by configuration-dependent pairing. The transition strengths  $B(E2)$  values that we obtained show that these structures are indeed collective and are deformed. This is confirmed by comparing them with the  $B(E2)$  values ( $1.35 e^2b^2$ ,  $1.35 e^2b^2$  and  $1.67 e^2b^2$ ) of the excited  $2_1^+$  state in the isotones  $^{150}\text{Sm}$ ,  $^{148}\text{Nd}$  and  $^{152}\text{Gd}$  respectively, these are very comparable [12].

### 4. Conclusion

The high spin measurements with AFRODITE have led to the discovery of new non-yrast structures and allowed lifetime estimates to be made in the nucleus  $^{150}\text{Sm}$ . The  $0_2^+$  band has been established to a spin-parity of  $12^+$ . Additionally, experimental lifetimes for the  $20^+$  and  $22^+$  states of the S-band 3 have been measured following the target thickness estimates. The preliminary lifetime measurements enabled the  $B(E2)$  values to be calculated. This analysis supported the more strongly collective interpretation of these states. This work support further measurements where in order to have a best fit for lifetime, relative target thickness should be evaluated every shift together with registration of the average beam current during the experiment, and  $45^\circ$  spectra should also be collected in order to minimize the uncertainty in the measurements.

#### 4.1. Acknowledgments

We would like to thank all our many colleagues in the AFRODITE group and students for their participation in the experiment and for the allocation of beam time at iThemba LABS.

#### References

- [1] Casten, R. F. and Zamfir, N. V., Phys. Rev. Lett. **47**, 1433 (1981).
- [2] R. F. Casten and P. Von Brentano and K. Heyde and P. Van Isacker and J. Jolie, Nucl. Phys. A **439**, 289 (1985).
- [3] D. C. Radford, Nucl. Instr. Methods Phys. Res. Sect. A **306**, 297 (1995).
- [4] Srebrny and Ch. Droste and T. Morek and K. Starosta and A. A. Wasilewski and A. A. Pasternak *et al.*, Nucl. Phys. A **683**, 21 (2001).
- [5] W. Urban and J. C. Barcelá and J. Nyberg, ACTA. Phys. Pol. **32**, 2527 (2001).
- [6] S.P. Bvumbi, J. F. Sharpey-Schafer, P. M. Jones, S. M. Mullins *et al.*, Phys. Rev. C **87**, 044333 (2013).
- [7] K. S. Krane and R. M. Steffen and R. M. Wheeler, Nucl. Data Tables A **11**, 351 (1973).
- [8] P. J. Twin, Nucl. Instr. Methods **106**, 481 (1973).
- [9] K. E. G. Löbner and M. Vetter and V. Hönig, Nucl. Data Tables, **47**, 495 (1970).
- [10] P. A. Aguer and C. F. Liang and J. Libert and P. Paris and A. Peghaire and A. Charvet and R. Duffait and G. Marguier, Nucl. Phys. A **252**, 293 (1975).
- [11] J. F. Sharpey-Schafer and S. M. Mullins and R. A. Bark and J. Kau and F. Komati and E. A. Lawrie and J. J. Lawrie and T. E. Madiba and P. Maine and A. Minkova and S. T. H. Murray and N. J. Ncapayi and P. A. Vymers, Eur. Phys. J. A **47**, 5 (2011).
- [12] S. Raman and C. W. Nestor JR. and P. Tikkanen, Atm. Data. and Nucl. Data. Tables **78**, 1-128 (2001).